An experimental study for rate constants of the gas phase reactions of CH_3CH_2OOH with OH radicals, O_3, NO_2 and NO

Caixia Wang, Zhongming Chen[*]

The State Key Laboratory of Environmental Simulation and Pollution Control, College of Environmental Sciences and Engineering, Peking University, Beijing 100871, China

ARTICLE INFO

ABSTRACT

The rate constants for ethyl hydroperoxide (EHP, CH_3CH_2OOH) reactions with OH radicals, O_3, NO_2 and NO in the gas phase have been investigated, by use of *in situ* long-path Fourier transform infrared spectroscopy. At 293 ± 2 K temperature and 760 Torr pressure, the measured values are $k_{EHP+OH} = (5.92 \pm 0.36) \times 10^{-12}$, $k_{EHP+O_3} \leq (8.4 \pm 0.1) \times 10^{-21}$, $k_{EHP+NO_2} \leq (9.7 \pm 0.3) \times 10^{-21}$ and $k_{EHP+NO} \leq (1.2 \pm 0.1) \times 10^{-21}$ cm^3 $molecule^{-1}$ s^{-1}. The atmospheric lifetimes of EHP with respect to these reactions have been estimated from these values, and the atmospheric implications have been briefly discussed.

1. Introduction

With increased understanding of atmospheric oxidation chemistry, the importance of organic peroxides in the VOC (volatile organic compound) transformation in the troposphere by the chemical processes of photolysis, reaction with the hydroxyl (OH) radical, reaction with the nitrate (NO_3) radical during evening and night time hours, reaction with O_3, and in coastal and marine areas reaction with Cl atoms during daylight hours (Atkinson and Arey, 2003), is becoming increasingly apparent. This is one of the most critical questions regarding atmospheric photochemical processes, because organic peroxides serve as both sinks and temporary reservoirs for important oxidants including HO_x (OH and HO_2) radicals and O_3 (Madronich and Calvert, 1990; Lightfoot et al., 1992). For example, it has been suggested that the photolysis of organic peroxides from the lower troposphere can provide a significant source of HO_x in the upper troposphere (Prather and Jacob, 1997; Wennberg et al., 1998; Matthews et al., 2005). Among these organic peroxides, methyl hydroperoxide (MHP, CH_3OOH)

and ethyl hydroperoxide (EHP, CH_3CH_2OOH) have been detected as two major constituents (Gunz and Hoffmann, 1990; Jackson and Hewitt, 1996; Lee et al., 2000; Sauer et al., 2001). Under favorable photochemical conditions, the atmospheric concentrations approach the ppbv (parts per billion by volume) level for MHP and EHP (Hewitt and Kok, 1991; Heikes et al., 1996; Weller et al., 2000; Grossmann et al., 2003; Xu et al., 2005).

Concentrations of these organic peroxides in the atmosphere depend not only on their sources, but also on their chemical conversions, which determine their sinks. To date, their chemical conversions in the atmosphere are poorly understood. A number of studies on the atmospheric chemical reactions of MHP have been carried out (Lightfoot et al., 1992; Vaghjiani et al., 1989; Thelen et al., 1993; Niki et al., 1983; Wallington et al., 1990; Chen and Wang, 2006; Wang and Chen, 2006), whilst there are only a few experimental studies on EHP (Wallington et al., 1989; Baulch et al., 1992) which include its photolysis and oxidation by Cl atoms. The atmospheric loss pathways of EHP probably include photolysis and reaction with oxidants such as OH radicals, NO_3 radicals, Cl atoms, O_3 and NO_x (NO_2 and NO). The atmospheric lifetime of EHP depends on the rates of these reactions and the concentration of

* Corresponding author. Tel.: +86 10 62751920; fax: +86 10 62751927.
E-mail address: zmchen@pku.edu.cn (Z. Chen).

oxidants. However, as far as we know, there are no published experimental data on the rate constants for the reactions of EHP with OH radicals, NO_3 radicals, O_3 and NO_x. In order to completely understand the atmospheric fate of EHP, better understanding of the kinetics of reactions of EHP with all five oxidants is required.

In this paper, we report the first investigation of the kinetics of EHP reactions with OH radicals, O_3 and NO_x, using *in situ* long-path Fourier transform infrared (LP-FTIR) spectroscopy. The objectives of this work were to obtain the rate constants. Finally, a comparison of the importance of different atmospheric decay process for EHP is performed.

2. Experimental methods

2.1. Reagents and instruments

Cyclohexane ($\geq$99.5%), *meta*-xylene ($\geq$99%), mesitylene ($\geq$99.9%), NO_2 (3400 ppmv diluted in N_2), NO (307 ppmv diluted in N_2) (China Research Center for Standard Compounds), N_2 ($\geq$99.999%) and O_2 ($\geq$99.999%) were used in this study. Ethyl hydroperoxide is not commercially available. It was synthesized by ethylation of hydrogen peroxide according to procedures described by Vaghjiani et al. (1989) and Lee et al. (2000). The purity of EHP was confirmed to be $\geq$97% by FTIR spectroscopy.

Simulation experiments were carried out in a 28.5 L quartz reaction chamber (Infrared Analysis Inc., USA). An FTIR spectrometer (Nexus model, Thermo Nicolet, USA) was used to observe the concentration changes of reactants and products. The reaction chamber was equipped with a digital thermometer, a piezometer to measure the gas pressure, a vacuum system and a White-mirror system. The instrument was described in detail in our previous work (Chen et al., 2003). There were five UV lamps ($\lambda_{max} = 254$ nm, 40 W) and a stainless steel enclosure around the reactor. FTIR spectra were recorded by co-adding 64 scans at 1 cm^{-1} spectral resolution throughout the frequency region of 500–4000 cm^{-1}. Temperature was controlled at 293 ± 2 K, while the total pressure of the gas mixture was controlled at 760 ± 10 Torr.

2.2. Investigation of the wall effect

In order to reduce the interference from the wall effect, the quartz reaction chamber was deactivated with OH radicals (the generation method for OH radicals is discussed below) for more than 12 h beforehand.

Attenuation experiments of the reactants (EHP, O_3, NO_2 and NO) in pure N_2 were performed separately to study the wall effect. Impurities and heterogeneous reactions possibly lead to the formation of OH radicals that will impact on the accuracy of the kinetic measurements. Therefore, cyclohexane was added to the reactant/N_2 system to trace OH radicals (the reactant represents EHP or O_3 or NO_2 or NO). Finally, the reaction chamber was kept in the dark for 5 h to investigate the change of cyclohexane in the chamber, which was used to trace the OH formation and *in situ* FTIR spectra were recorded to observe the change in the mixture system.

2.3. OH reaction with EHP

In this study, OH radicals were generated by UV photolysis of O_3 in the presence of water vapor:

$$O_3 + h\nu \rightarrow O(^1D) + O_2 \tag{1}$$

$$O(^1D) + H_2O \rightarrow 2OH \tag{2}$$
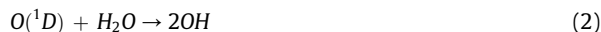
The relative rate method was employed to determine the reaction rate constant of EHP with OH radicals. First, we select cyclohexane, which is an accepted competitive reactant for the OH reaction with organics, as the reference. Additionally, *meta*-xylene and mesitylene were also selected as references for further investigation of the rate constant of the OH reaction with EHP. These three references do not photolyze under the experimental conditions and their oxidation by OH radicals will not produce EHP. Furthermore, the reaction rate constants of these references with OH radicals have been well studied and the results from different groups are almost identical.

In the reactor, EHP will compete with the reference (denoted by Ref) to react with OH radicals, and the concentration relationship between EHP and reference can be expressed as

$$\ln\frac{[EHP]_{t0}}{[EHP]_t} = \frac{k_{EHP-OH}}{k_{Ref-OH}} \ln\frac{[Ref]_{t0}}{[Ref]_t} \tag{3}$$

where, k_{Ref-OH} and k_{EHP-OH} are the corresponding second-order rate constants, $[EHP]_{t0}$ and $[Ref]_{t0}$ are the initial concentrations of EHP and the reference, and $[EHP]_t$ and $[Ref]_t$ are concentrations of EHP and the reference at the reaction time t. Using FTIR for the *in situ* investigation of the decrease of EHP and references, combined with the reaction rate constants of the references with OH radicals, we can calculate the reaction rate constant of EHP with OH radicals from Eq. (3).

During the experiment, water, EHP and reference were introduced into the evacuated reactor in turn. After these three compounds had been evaporated completely, O_3, which was generated in a 2.8 L quartz chamber beforehand, was added, followed by synthesized air (O_2:N_2 = 1:4, i.e. the experiment was carried out under simulated atmospheric conditions) to reach a pressure of 760 Torr. After the gases were mixed homogenously, the UV lamps were turned on and the *in situ* FTIR spectra were recorded to determine the concentration changes of EHP and the reference. The initial gaseous concentrations were $(1.48 \pm 0.09) \times 10^{15}$ molecule cm^{-3} of EHP and $(9.84 \pm 0.79) \times 10^{16}$ molecule cm^{-3} of water vapor. The absorption wavenumbers used for detection of EHP, cyclohexane, *meta*-xylene, and mesitylene were selected at 1337, 2862, 769, and 836 cm^{-1}, respectively.

In order to subtract the photolysis effect on EHP reaction with OH radicals in the reactor, we carried out two reaction systems. First, the concentrations of EHP and reference before and during the reaction, i.e. $[EHP]'_{t0}$, $[Ref]_{t0}$, $[EHP]'_t$ and $[Ref]_t$, were determined for the simultaneous reaction of EHP and reference with OH radicals (reaction system I). In this reaction system, the UV photolysis of EHP also contributes to the decay of EHP because of the existence

of UV radiation. It is necessary to take the UV photolysis reaction into account. Therefore, we measured the concentration variation of EHP for the UV photolysis reaction of EHP in N_2 (reaction system II). The fractional variation of EHP at different times in reaction system II was calculated and this value was added to the EHP concentration detected in reaction system I in order to obtain the actual concentration of EHP at the corresponding time ($[EHP]_t$). This adjustment corrected for the complication caused by the photolysis reaction.

2.4. O_3 and NO_x reactions with EHP

In the reaction system of EHP with XO (here $XO = O_3$, NO_2, and NO), if the concentration of XO is in excess of EHP or if the percentage conversion of XO is less than 15%, the concentration of XO can be assumed to be constant during the reaction. Then, we can obtain

$$\ln\frac{[EHP]_t}{[EHP]_{t0}} = -k^{1st}t \qquad (4)$$

where k^{1st} is a pseudo-first-order rate constant which is independent of the EHP concentration, $k^{1st} = k[XO]$, t is the reaction time and $[EHP]_{t0}$ and $[EHP]_t$ are the concentrations of EHP at the beginning and at the reaction time t, respectively. Under these conditions, the natural logarithm (ln) of $([EHP]_{t0}/[EHP]_t)$ was plotted against the reaction time, and the pseudo-first-order rate coefficient, k^{1st}, was the slope of the straight line fitted to the experimental data.

During the experiment, the pure EHP liquid was first introduced into the evacuated reactor without light. After it had evaporated completely, gaseous O_3 (which was generated in 2.8 L quartz chamber beforehand) or NO_2 or NO was added, followed by pure N_2 or synthesized air to reach atmospheric pressure.

3. Results and discussion

3.1. Wall effect

The results of the attenuation experiment indicated that in the reactor the decay rates of gaseous EHP, O_3, NO_2 and NO were about 1% h^{-1} of their initial concentrations. Also, as mentioned above, the quartz reaction chamber was deactivated with OH radicals beforehand. In the reactant/cyclohexane/N_2 system, cyclohexane is a tracer for OH radicals. The result showed that there was no obvious variation in the concentration of cyclohexane in the chamber, and this suggests that no significant formation of OH radicals occurred there. Furthermore, no new products were detected according to the FTIR spectra. Therefore, the impact of impurities and heterogeneous reactions is negligible.

3.2. Rate constant of the OH reaction with EHP

According to the calculation, the magnitude of photolysis loss was about one-seventh of the OH reaction loss. Next, the kinetic curve of the concentration variation of EHP was drawn. The relationship between $\ln([EHP]_{t0}/$

$[EHP]_t)$ and $\ln([Ref]_{t0}/[Ref]_t)$ is illustrated in Fig. 1 and a linear least-squares fit was calculated. All the correlation coefficients (R^2) are larger than 0.99. The results with different references are listed in Table 1. The average value was taken as the rate constant of the EHP reaction with OH radicals, which is $(5.92 \pm 0.36) \times 10^{-12}$ cm^3 molecule^{-1} s^{-1}.

It is noticed that $O(^1D)$ atoms produced by UV photolysis of O_3 can react with EHP and other reagents. However, due to the high H_2O concentration of $(9.84 \pm 0.79) \times 10^{16}$ molecule cm^{-3}, $O(^1D)$ reacted mainly with H_2O to produce OH radicals (DeMore, 1992; Chen et al., 1997). Thus the dynamic concentration of $O(^1D)$ was very low and its reaction with EHP was negligible.

To date, we are unaware of any experimental study on the rate constant of the EHP reaction with OH radicals. The only published data were recommended by analogy with the rate constant of the MHP reaction with OH radicals, with the value of 5.74×10^{-12} cm^3 molecule^{-1} s^{-1} at 293 K (Baulch et al., 1992). This value is closed to the result of our study. The fact that methyl and ethyl hydroperoxides seem to have nearly the same OH rate constant implies that H-abstraction from the –OOH group may be the dominant channel for the OH reactions of organic hydroperoxides.

3.3. Rate constant of the O_3 reaction with EHP

From the FTIR spectra, we can identify the major absorption bands of EHP at 3598, 2994, 2934, 1337, 1043 and 831 cm^{-1}. The absorption band at 1337 cm^{-1} was used for quantitative measurement of EHP. From the subtraction analysis of the FTIR absorption spectra, CH_3OH, HCHO, HCOOH, C_2H_5OH and CH_3CHO were identified as the main products.

In the reaction time allowed, the percentage conversion of O_3 was less than 15%, thus the concentration variation of EHP was treated as a pseudo-first-order reaction. The dependence of $\ln([EHP]_{t0}/[EHP]_t)$ on reaction time is shown in Fig. 2. As for the first-order reaction, the rate constant can be obtained from Eq. (4). Values of the first-order rate
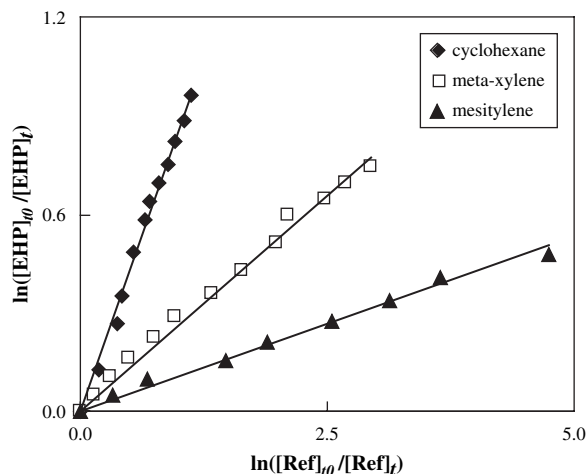

Fig. 1. Plots of the concentration relationship for determination of the reaction rate constant of EHP with OH radicals. The lines are fitted using a least-squares routine.

Table 1
Reaction rate constant of EHP with OH

Reference	$[Ref]_{t0}$ (10^{15} molecule cm^{-3})	$[EHP]_{t0}$ (10^{15} molecule cm^{-3})	k_{Ref-OH} (10^{-12} cm^3 molecule^{-1} s^{-1})	k_{EHP-OH}/k_{Ref-OH}	k_{EHP-OH} (10^{-12} cm^3 molecule^{-1} s^{-1})
Cyclohexane	1.97 ± 0.10	1.48 ± 0.09	6.84[a]	0.859 ± 0.024	5.88 ± 0.16
meta-Xylene	1.48 ± 0.07	1.48 ± 0.09	22.0[b]	0.264 ± 0.013	5.81 ± 0.29
Mesitylene	1.48 ± 0.07	1.48 ± 0.09	57.3[b]	0.106 ± 0.009	6.07 ± 0.52
Average value					5.92 ± 0.36

[a] Atkinson, 2003.
[b] Kramp and Paulson, 1998.

coefficients for the loss of EHP in the absence and presence of O$_3$, i.e. k_{EHP}^{w} and k'_{EHP-O_3}, were thus determined as $(5.0 \pm 0.1) \times 10^{-6}$ s^{-1} and $(2.06 \pm 0.02) \times 10^{-5}$ s^{-1}, respectively. Taking k_{EHP}^{w} into account, the first-order rate coefficient of the EHP with O$_3$ ($k_{EHP-O_3}^{1st}$) is

$$k_{EHP-O_3}^{1st} = k'_{EHP-O_3} - k_{EHP}^{w} = (1.56 \pm 0.02) \times 10^{-5} \text{ s}^{-1} \quad (5)$$

From this, an absolute value of the second-order rate constant (k_{EHP-O_3}) was derived,

$$k_{EHP-O_3} = k_{EHP-O_3}^{1st}/[O_3]$$
$$= (8.4 \pm 0.1) \times 10^{-21} \text{ cm}^3 \text{ molecule}^{-1} \text{ s}^{-1} \quad (6)$$

where [O$_3$] represents the average concentration of O$_3$ (1.40×10^{15} molecule cm^{-3}) during the reaction period.

According to the result of the wall effect experiment, the heterogeneous reaction seems to be negligible. However, because the change of the wall loss of EHP in the presence of O$_3$ cannot be completely excluded, the value in Eq. (6) should be considered as the upper limit to the bimolecular rate constant of the EHP–O$_3$ reaction.

3.4. Rate constant of the NO$_2$ reaction with EHP

From analysis of the FTIR spectra, CH$_3$CH$_2$ONO$_2$ is identified as the major product during the reaction of NO$_2$ with EHP. Moreover, a decrease of both EHP and NO$_2$ was observed and a detailed analysis of the FTIR spectra shows no evidence of other organic nitrates.
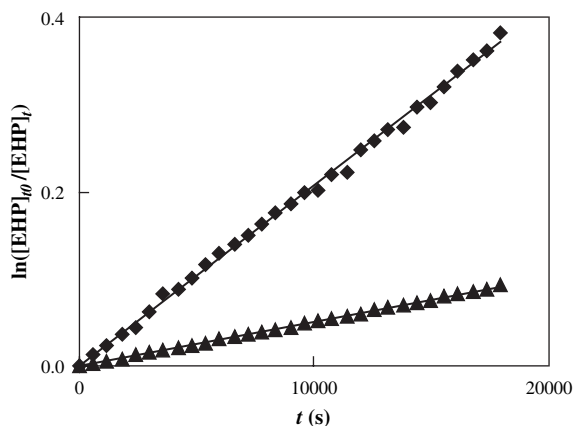
On the basis of the absorbance of EHP at different reaction times, straight lines were obtained for plots of ln($[EHP]_{t0}/[EHP]_t$) and the reaction time (Fig. 3). Different symbols indicate that the initial concentrations of NO$_2$ were $(1.58 \pm 0.08) \times 10^{15}$ and $(2.14 \pm 0.11) \times 10^{15}$ molecule cm^{-3}, respectively. The pseudo-first-order rate constant, k'_{EHP-NO_2}, can be calculated from Eq. (4) as $(2.04 \pm 0.04) \times 10^{-5}$ s^{-1} and $(2.57 \pm 0.03) \times 10^{-5}$ s^{-1}, respectively. The solid squares in Fig. 3 describe the loss of EHP on the wall of the quartz reactor in the absence of NO$_2$. The wall loss of EHP (k_{EHP}^{w}) was determined to be $(5.10 \pm 0.01) \times 10^{-6}$ s^{-1}.

Taking k_{EHP}^{w} into account, the first-order rate coefficient of the EHP with NO$_2$ ($k_{EHP-NO_2}^{1st}$) is

$$k_{EHP-NO_2}^{1st} = k'_{EHP-NO_2} - k_{EHP}^{w} \quad (7)$$

Then, the value of the second-order rate constant (k_{EHP-NO_2}) can be derived from the following equation:

$$k_{EHP-NO_2} = k_{EHP-NO_2}^{1st}/[NO_2] \quad (8)$$

The average value at different NO$_2$ initial concentrations was taken as the rate constant of EHP with NO$_2$, which is $(9.7 \pm 0.3) \times 10^{-21}$ cm^3 molecule^{-1} s^{-1}. This value should be considered as the upper limit to the bimolecular rate constant of the EHP–NO$_2$ reaction, because the change of the wall loss of EHP in the presence of NO$_2$ cannot be completely excluded.
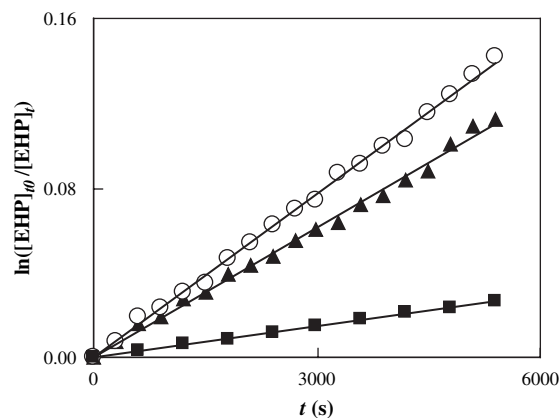

Fig. 2. Plots of ln($[EHP]_{t0}/[EHP]_t$) vs. reaction time in the reaction of EHP in the presence or absence of O$_3$. ▲ EHP–air, ◆ EHP–O$_3$–air. The lines are fitted using a least-squares routine.

Fig. 3. Plots of ln($[EHP]_{t0}/[EHP]_t$) vs. reaction time in the reaction of EHP with NO$_2$. The initial concentration of NO$_2$ was (▲) 1.58×10^{15}, (○) 2.14×10^{15} molecule cm^{-3}. (■) shows the wall loss of EHP alone. The lines are fitted using a least-squares routine.

To our surprise, $CH_3CH_2ONO_2$ is identified as the major product of the EHP–NO_2 reaction in the dark. However, its formation mechanism is unclear.

3.5. Rate constant of the NO reaction with EHP

In order to further elucidate the loss pathway of EHP with special regard to NO_x, the reaction of EHP with NO was also investigated in the dark. This experiment lasted for 90 min and the result revealed that there was no distinct variation in EHP and no other products were found. Based on the value of $k_{EHP}^{w} = (5.10 \pm 0.01) \times 10^{-6}\ s^{-1}$ and the concentration of NO, $(4.43 \pm 0.22) \times 10^{15}$ molecule cm^{-3}, the second-order rate constant of the reaction of EHP with NO can be derived as

$$k_{EHP-NO} \leq k_{EHP}^{w}/[NO]$$
$$= (1.2 \pm 0.1) \times 10^{-21}\ cm^3\ molecule^{-1}\ s^{-1}. \qquad (9)$$

4. Conclusions

The results presented here represent the first experimental measurement of the reaction rate constants of EHP with OH radicals, O_3, NO_2 and NO. The results are summarized in Table 2.

The chemical processes that remove EHP from the atmosphere are possibly its photolysis and its reactions with oxidants such as OH radicals, O_3 and NO_x. The oxidants also include Cl atoms in the marine and coastal boundary layer and NO_3 radicals at night time. Therefore, the EHP concentration is controlled by the mixing ratios of these oxidants and the solar radiation intensity. The atmospheric lifetimes of EHP can be estimated with respect to these loss reactions, based on the corresponding rate constants and the estimated ambient tropospheric concentrations of these reactive species, according to Eq. (10):

$$\tau_{EHP-XO} = \frac{1}{k_{EHP-XO}[XO]} \qquad (10)$$

where k_{EHP-xO} is the rate constant and $[XO]$ is the estimated ambient concentration of an oxidant. The rate constants

measured in the present work were k_{EHP-xO} for the reactions of EHP with OH radicals, O_3 and NO_2, while the rate constants corresponding to Cl atoms and photolysis reactions were obtained from previous studies (Wallington et al., 1989; Baulch et al., 1994). The rate constant for the EHP reaction with NO_3 radicals is not available, thus the related lifetime is not discussed. Results are listed in Table 2.

As shown in Table 2, the atmospheric lifetimes of EHP with respect to its photolysis and reactions with OH radicals, O_3 and NO_2 were estimated at 6.8 days, 2.4 days, more than 3.0 years and more than 2.6 years, respectively. During the day, solar radiation is present and higher OH concentrations occur accompanied by higher concentrations of O_3 and NO_2 compared with those at night time, thus the variation in rate of EHP loss will be complex. However, even in heavily polluted air (NO_2 level up to 100 ppbv), the NO_2–EHP reaction is about 400 times slower than the OH–EHP reaction, so that the removal of EHP by NO_2 accounts for only a few percent of the total daytime EHP loss. A similar situation occurs for the removal of EHP by O_3. Thus, the direct reactions with O_3 and NO_2 are likely to be a negligible sink for EHP, and the overall daytime lifetime of EHP is mainly determined by its reaction with OH radicals and its photolysis in daytime, and typically will be about 2.4 days in a typical boundary layer. Based on such a lifetime, it is likely that EHP can be transported to the upper troposphere under strong convective weather conditions. Of course, in the marine boundary layer, a contribution to the conversion of EHP by Cl atom oxidation needs further consideration. Furthermore, in order to quantify the night time loss of EHP, the NO_3/N_2O_5 chemistry needs to be studied in the future.

Acknowledgements

References

Atkinson, R., 2003. Kinetics of the gas-phase reactions of OH radicals with alkanes and cycloalkanes. Atmospheric Chemistry and Physics 3 (6), 2233–2307.

Atkinson, R., Arey, J., 2003. Atmospheric degradation of volatile organic compounds. Chemical Reviews 103 (12), 4605–4638.

Baulch, D.L., Cobos, C.J., Cox, R.A., Esser, C., Frank, P., Just, T., Kerr, J.A., Pilling, M.J., Troe, J., Walker, R.W., Warnatz, J., 1992. Evaluated kinetic data for combustion modeling. Journal of Physical and Chemical Reference Data 21 (3), 411–429.

Baulch, D.L., Cobos, C.J., Cox, R.A., Frank, P., Hayman, G., Just, T., Kerr, J.A., Murrells, T., Pilling, M.J., Troe, J., Walker, R.W., Warnatz, J., 1994. Evaluated kinetic data for combustion modeling. Journal of Physical and Chemical Reference Data 23 (6), 847–1033.

Chen, Z.M., Li, S., Shi, F., Tang, X.Y., 2003. Study on the yield of peroxides from atmospheric reaction of $CH_3C(O)CH=CH_2$ with O_3 by Long Path FTIR. Spectroscopy and Spectral Analysis 23 (4), 742–744.

Chen, Z.M., Wang, C.X., 2006. Rate constants of the gas-phase reactions of CH_3OOH with O_3 and NO_x at 293 K. Chemical Physics Letters 424 (4–6), 233–238.

Chen, Z.M., Zhang, Y.H., Tang, X.Y., Li, J.L., 1997. The study of reaction rate constants of CFCs with OH radicals using long path spectrometry. China Environmental Science 17 (1), 41–44.

Table 2
Reaction rate constants and atmospheric lifetimes of EHP

Reactants	Concentration (molecule cm^{-3})	k (293 K) (cm^3 molecule^{-1} s^{-1})	τ (days)
OH	1.6×10^6 [d]	5.92×10^{-12} [a]	2.4
Photolysis	–	$3.4 \times 10^{-6}\ s^{-1}$ [b]	6.8
Cl	3.0×10^4 [e]	1.1×10^{-10} [c]	7.0
O_3	2.5×10^{12} [f]	$\leq 8.4 \times 10^{-21}$ [a]	$\geq 1.1 \times 10^3$
NO_2	2.5×10^{12} [g]	$\leq 9.7 \times 10^{-21}$ [a]	$\geq 9.5 \times 10^2$

[a] This work.
[b] Baulch et al., 1994.
[c] Wallington et al., 1989.
[d] 12 h Daytime average concentration of OH radicals in the troposphere.
[e] 12 h Daytime average concentration of Cl atoms in the marine boundary layer.
[f] Peak concentration of O_3 in heavily polluted air.
[g] Peak concentration of NO_2 in heavily polluted air.

DeMore, W.B., 1992. Relative rate constants for the reactions of OH with methane and methyl chloroform. Geophysical Research Letters 19 (13), 1367–1370.

Grossmann, D., Moortgat, G.K., Kibler, M., Schlomski, S., Bachmann, K., Alicke, B., Geyer, A., Platt, U., Hammer, M.U., Vogel, B., Mihelcic, D., Hofzumahaus, A., Holland, F., Volz-Thomas, A., 2003. Hydrogen peroxide, organic peroxides, carbonyl compounds, and organic acids measured at Pabstthum during BERLIOZ. Journal of Geophysical Research 108 (D4) PHO 6–1.

Gunz, D.W., Hoffmann, M.R., 1990. Atmospheric chemistry of peroxides: a review. Atmospheric Environment 24A (17), 1601–1633.

Heikes, B., Lee, M.H., Jacob, D., Talbot, R., Bradshaw, J., Singh, H., Blake, D., Anderson, B., Fuelberg, H., Thompson, A.M., 1996. Ozone, hydroperoxides, oxides of nitrogen, and hydrocarbon budgets in the marine boundary layer over the South Atlantic. Journal of Geophysical Research 101 (D19), 24221–24234.

Hewitt, C.N., Kok, G.L., 1991. Formation and occurrence of organic hydroperoxides in the troposphere: laboratory and field observations. Journal of Atmospheric Chemistry 12 (2), 181–194.

Jackson, A.V., Hewitt, C.N., 1996. Hydrogen peroxide and organic hydroperoxide mixing ratio in air in a eucalyptus forest in central Portugal. Atmospheric Environment 30 (6), 819–830.

Kramp, F., Paulson, S.E., 1998. On the uncertainties in the rate coefficients for OH reactions with hydrocarbons, and the rate coefficients of the 1,3,5-trimethylbenzene and *m*-xylene reactions with OH radicals in the gas phase. Journal of Physical Chemistry A 102 (16), 2685–2690.

Lee, M., Heikes, B.G., O'Sullivan, D.W., 2000. Hydrogen peroxide and organic hydroperoxide in the troposphere: a review. Atmospheric Environment 34 (21), 3475–3494.

Lightfoot, P.D., Cox, R.A., Crowley, J.N., Destriau, M., Hayman, G.D., Jenkin, M.E., Moortgat, G.K., Zabel, F., 1992. Organic peroxy radicals: kinetics, spectroscopy and tropospheric chemistry. Atmospheric Environment 26 (10), 1805–1961.

Madronich, S., Calvert, J.G., 1990. Permutation reactions of organic peroxy radicals in the troposphere. Journal of Geophysical Research 95 (D5), 5697–5715.

Matthews, J., Sinha, A., Francisco, J.S., 2005. The importance of weak absorption features in promoting tropospheric radical production. Proceedings of the National Academy of Sciences of the United States of America 102 (21), 7449–7452.

Niki, H., Maker, P.D., Savage, C.M., Breitenbach, L.P., 1983. A fourier transform infrared study of the kinetics and mechanism for the reaction $HO + CH_3OOH$. Journal of Physical Chemistry 87 (12), 2190–2193.

Prather, M.J., Jacob, D.J.A., 1997. A persistent imbalance in HO_x and NO_x photochemistry of the upper troposphere driven by deep tropical convection. Geophysical Research Letters 24 (24), 3189–3192.

Sauer, F., Beck, J., Schuster, G., Moortgat, G.K., 2001. Hydrogen peroxide, organic peroxides and organic acids in a forested area during FIELD-VOC'94. Chemosphere – Global Change Science 3 (3), 309–326.

Thelen, M.A., Felder, P., Huber, J.R., 1993. The photo fragmentation of methyl hydroperoxide CH_3OOH at 193 and 248 nm in a cold molecular-beam. Chemical Physics Letters 213 (3–4), 275–281.

Vaghjiani, G.L., Ravishankara, A.R., Cohen, N., 1989. Kinetics and mechanism of OH reaction with CH_3OOH. Journal of Physical Chemistry 93 (5), 1948–1959.

Wallington, T.J., Andino, J.M., Ball, J.C., Japar, S.M., 1990. Fourier transform infrared studies of the reaction of Cl atoms with PAN, PPN, CH_3OOH, HCOOH, CH_3COCH_3 and $CH_3COC_2H_5$ at 295 ± 2 K. Journal of Atmospheric Chemistry 10 (3), 301–313.

Wallington, T.J., Gierczak, C.A., Ball, J.C., Japar, S.M., 1989. Fourier transform infrared study of the self reaction of $C_2H_5O_2$ radicals in air at 295 K. International Journal of Chemical Kinetics 21 (11), 1077–1089.

Wang, C.X., Chen, Z.M., 2006. Effect of CH_3OOH on the atmospheric concentration of OH radicals. Progress in Natural Science 16 (11), 1141–1149.

Weller, R., Schrems, O., Boddenberg, A., Gäb, S., Gautrois, M., 2000. Meridional distribution of hydroperoxides and formaldehyde in the marine boundary layer of the Atlantic (48 degrees N–35 degrees S) measured during the Albatross campaign. Journal of Geophysical Research 105 (D11), 14401–14412.

Wennberg, P.O., Hanisco, T.F., Jaegle, L., Jacob, D.J., Hintsa, E.J., Lanzendorf, E.J., Anderson, J.G., Gao, R.S., Keim, E.R., Donnelly, S.G., Del Negro, L.A., Fahey, D.W., McKeen, S.A., Salawitch, R.J., Webster, C.R., May, R.D., Herman, R.L., Proffitt, M.H., Margitan, J.J., Atlas, E.L., Schauffler, S.M., Flocke, F., McElroy, C.T., Bui, T.P., 1998. Hydrogen radicals, nitrogen radicals, and the production of O_3 in the upper troposphere. Science 279 (5347), 49–53.

Xu, J.R., Chen, Z.M., Wang, C.X., Luo, Z.M., Zhang, Y.H., Zeng, L.M., 2005. Atmospheric measurements of hydrogen peroxide and organic hydroperoxides in Guangzhou Urban during PRD Intensive Campaign 2004. Proceedings of Scientific Assembly of the International Association of Meteorology and Atmospheric Sciences, Beijing, China, 2–11 August.